PCCP

PAPER

View Article Online
View Journal | View Issue



Cite this: *Phys. Chem. Chem. Phys.*, 2022, **24**, 2966

# Circularly polarized light-induced potentials and the demise of excited states

Sebastián Carrasco,[a] José Rogan,[bc] Juan Alejandro Valdivia,[bc] Bo Y. Chang,[d] Vladimir S. Malinovsky[a] and Ignacio R. Sola[*e]

Received 3rd October 2021,
Accepted 28th December 2021

DOI: 10.1039/d1cp04523g

rsc.li/pccp

In the presence of strong electric fields, the excited states of single-electron molecules and molecules with large transient dipoles become unstable because of anti-alignment, the rotation of the molecular axis perpendicular to the field vector, where bond hardening is not possible. We show how to overcome this problem by using circularly polarized electromagnetic fields. Using a full quantum description of the electronic, vibrational, and rotational degrees of freedom, we characterize the excited electronic state dressed by the field and analyze its dependence on the bond length and angle and the stability of its vibro-rotational eigenstates. Although the dynamics is metastable, most of the population remains trapped in this excited state for hundreds of femtoseconds, allowing quantum control. Contrary to what happens with linearly polarized fields, the photodissociation occurs along the initial molecular axis, not perpendicular to it.



## 1 Introduction

The quantum treatment of the dynamics of a molecule in all its degrees of freedom is an imposing computational challenge. Owing to the hierarchy of masses and the consequent different scales of motion, for coupled degrees of freedom one often describes each slower motion based on the average potential created by the faster motion, reducing the dimensions of the problem.[1–5] In addition, it is customary to treat the nuclear (slower) motions using a classical or semiclassical approach. Such approximations do not allow one to describe the back-action of the slower motion on to the faster one, inducing decoherence, although the former effect can be approximately described by averaging over trajectories. In addition, when the time-scale of the motions is not very different, as at nuclear configurations where the electronic states are nearly degenerate (*e.g.* at conical intersections) and particularly with lighter atoms, the approximations are deemed to fail and a full quantum treatment is necessary. This is particularly the case for the hydrogen molecular cation and its isotopes. We have recently developed a model and computational scheme to integrate the time-dependent Schrödinger equation (TDSE) for one-electron molecules in 3-electronic plus 2-nuclear degrees of freedom (internuclear distance and angle of the molecular axis with respect to a fixed axis) in the presence of electromagnetic fields.[6]

The first excited state of $H_2^+$ or any other one-electron molecule is dissociative, corresponding to the anti-bonding character of its molecular orbital. However, under an electric field, the ground and first excited electronic states become mixed so that their corresponding dressed potentials feature bond softening[7–10] and bond hardening.[11–14] With field intensities of the order of or larger than TW/cm$^2$, bond hardening in the excited dressed potential is enough to support several bound vibrational states. Many quantum control schemes rely on bond hardening to control the bond length of molecules[15–19] to generate huge dipole moments,[20–22] or to control the photofragment velocity and angular distribution[23–26] requiring the previous alignment of the molecules with the external field.[27,28] Diatomic molecules can be aligned by means of different techniques, more so if the molecules have a permanent dipole, and a single strong non-resonant field (perhaps the same used for bond-hardening) can be used for this purpose. It is customary to assume that the molecules may remain aligned at least during the short period of time during which one acts on or control their dynamics with ultrafast laser pulses. While this is true in the ground state of the molecule, we recently found that the converse is the norm in the excited state,[29] even when the molecule had a permanent dipole moment and is subject to a constant electric field, as in $HD^+$.[6] Then, anti-alignment, that is, the alignment of the molecular axis perpendicular to the polarization of the field, moves the molecule out of the influence of the field in as short a time as a molecular vibration, leading to fast photodissociation.

Anti-alignment was first predicted using a semiclassical model, where the nuclear motion was treated classically, allowing

[a] *U.S. Army Research Laboratory, Adelphi, Maryland 20783, USA*
[b] *Departamento de Física, Facultad de Ciencias, Universidad de Chile, Casilla 653, Santiago 7800024, Chile*
[c] *Centro Para la Nanociencia y la Nanotecnolgía, CEDENNA, Chile*
[d] *School of Chemistry(RIBS), Seoul National University, Seoul 08826, Republic of Korea*
[e] *Departamento de Química Física, Universidad Complutense, 28040 Madrid, Spain. E-mail: isola@quim.ucm.es*

 

for bond-hardening in those molecules initially aligned with the field.[29] Therefore, one could anticipate a control mechanism relying on laser alignment in the ground state before sending the population to the excited potential dressed by a field or, alternatively, a control process that would filter those molecules initially aligned with the field, the only ones to survive after the excitation. But using a full quantum description, we observed that the angular width of the initial wave function is always enough to induce total dissociation.[6] In fact, aided by dephasing, a very narrow angular wave packet anti-aligns more rapidly than a wider distribution. The survival time in the excited state only depends on the average angle and not on the angular dispersion. In addition, the anti-alignment process was strong enough to beat the dipole-induced alignment when the molecule had an initial dipole moment, as in the $HD^+$ isotope. The question then is are all strong field control scenarios based upon bond hardening in the excited states doomed to fail?

When working with electromagnetic fields, rather than static or ac electric fields, we expect some differences to occur. The field frequency selects the geometry of the excited potential that is resonant with the ground potential, forcing a stronger reshaping of the light-induced potentials[30–35] (LIPs) and trapping population at selected internuclear distances in the excited state. This is not the case, however, when the molecular axis is perpendicular to the polarization and $\theta = \pi/2$. Then the coupling is zero and the molecule dissociates, while some population may be transferred to the ground potential by non-adiabatic processes in the vicinity of $\theta = \pi/2$. In the representation of the LIPs, this process can be seen as fast internal conversion through a light-induced conical intersection[35–41] or LICI, using the language of Photochemistry, and it is possible even in diatomic molecules, including the rotational degree of freedom. There have been a plethora of studies concerning how to probe the LICIs and how to use them as a resource to control photochemical or photophysical processes, but if anything, one expects that the presence of LICIs will make it harder to stabilize the excited states of single electron molecules.

But the frequency is not the only control knob that electromagnetic fields provide: one can use the vectorial properties of the field to control the dynamics *via* the polarization of light. The selection rules of different spectroscopic techniques crucially depend on whether one uses linearly or circularly polarized fields.[42,43] It is also well known that the polarization of the field directly affects the electronic motion, as observed for instance in the yields of ionization and high harmonic generation.[44] Although circularly polarized fields are often used as enantio-sensitive signals that probe the chirality of the media (*e.g.* in measurements of circular dichroism or in photo-electron currents upon ionization[45–48]) they have also been proposed to control the dynamics.[49,50] As an example, two pulses of circularly polarized light with different wavelengths could orient molecules,[51,52] although simpler schemes were suggested.[27,28] This is a field under development, as the technology of pulse shaping including the full vectorial properties of light is now available[53] and a further step is being taken for creating synthetic chiral light.[54]

In this work we show the effects and dynamics of antialignment with electromagnetic fields, rather than electric pulses, and study the role of polarization. Both by using a theoretical model and by solving the TDSE for the electronic, vibrational and rotational degrees of freedom, we find that bond hardening in the excited state of $H_2^+$ is stable (actually meta-stable) using circularly polarized fields. Hence, the molecule survives in the excited state for the duration of short pulses. In contrast, there is antialignment that leads to fast photodissociation when using linearly polarized fields, while the effect of elliptically polarized fields stands in between both extremes. In Section 2, we outline the theoretical model. In Section 3, we introduce the numerical method used to solve the TDSE. Section 4 discusses the dynamics and dissociation in the excited state under different initial conditions and fields, and finally, conclusions are provided in Section 5.

## 2 Theory: excited state stability under linear and circularly polarized fields

As previously outlined, a strong field can induce bond hardening in the first excited dressed state of $H_2^+$, enough to support several bound vibrational states, but the orientation of the molecular axis with the electric field makes such bond-hardening to be dependent on the nature of the polarization properties of light. To understand the origin of the stability or instability of the excited electronic state conditional to the polarization properties of the dressing field, we present here a model which allows one to predict the average properties of the light-induced potentials under certain approximations. This will be confronted with the numerical results in Section 4 which avoid the approximations.

Consider two isolated electronic states of a diatomic molecule (*e.g.* the ground $V_g(R)$ and the first excited state $V_e(R)$) that lies in the plane perpendicular to the axis of propagation of the field $\mathbf{e}_y$. In the length gauge and dipole approximation, the coupling with the external, linearly polarized field $\mathbf{E}_1(t)$ (see Fig. 1) adds the term

$$\mathbf{E}(t)\cdot\mathbf{r} = E_1(t)S(t)(\cos\theta\,\mathbf{e}_z + \sin\theta\,\mathbf{e}_x)\cdot(z\mathbf{e}_z + x\mathbf{e}_x) \quad (1)$$

$$= E_1 S(t) z\cos\theta \quad (2)$$

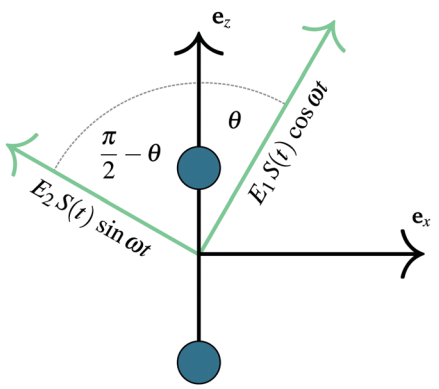


Fig. 1 Diagram of the $H_2^+$ molecule under an elliptically polarized field. The field can be understood as two perpendicular linearly polarized fields with different amplitudes that differ in phase by $\pi/2$.

where $S(t)$ is a slowly evolving (possibly constant) pulse envelope, $E_1$ the pulse peak amplitude, and $\theta$ the angle between the internuclear vector and the field. Note that we are omitting $x$ in eqn (2) because it is zero for the ground and first excited states of $H_2^+$. Bold letters are reserved for vectors. For an elliptically polarized field (two perpendicular linearly polarized fields with opposite phases)

$$\mathbf{E}(t)\cdot\mathbf{r} = zE_1S(t)\cos\theta\cos(\omega t) + zE_2S(t)\sin\theta\sin(\omega t) \qquad (3)$$

The potential energy matrix can be written as

$$V = \begin{pmatrix} V_g & 0 \\ 0 & V_u \end{pmatrix} + 2S(t)\mu(E_1\cos\theta\cos\omega t + E_2\sin\theta\sin\omega t)\sigma_x \qquad (4)$$

In the rotating frame, defined by

$$\psi_R = \exp\left(-\frac{i}{2}\omega t(\sigma_z - I)\right)\psi$$

the TDSE becomes

$$i\hbar\frac{d}{dt}\psi_R = H_R\psi_R = -\frac{1}{2}\hbar\omega\psi_R + \frac{1}{2}\hbar\omega\sigma_z\psi_R + \exp\left(-\frac{i}{2}\omega t\sigma_z\right)(T+V)\exp\left(+\frac{i}{2}\omega t\sigma_z\right)\psi_R$$

where we have used the $2\times 2$ Pauli matrices $\sigma_x$ and $\sigma_z$, and the unit matrix $I$, for notational convenience. Since we are interested in the potential energy dressed by the field, we will omit the kinetic energy operator $T$ from our consideration. In principle, a time-dependent transformation adds non-adiabatic terms to the kinetic energy, which are often neglected under the adiabatic approximation. Because of

$$\exp\left(-\frac{i}{2}\omega t\sigma_z\right)\sigma_x\exp\left(+\frac{i}{2}\omega t\sigma_z\right) = \begin{pmatrix} 0 & e^{-i\omega t} \\ e^{+i\omega t} & 0 \end{pmatrix}$$

we obtain

$$V_R = \begin{pmatrix} V_g & \mu S(t)(E_1\cos\theta - iE_2\sin\theta) \\ \mu S(t)(E_1\cos\theta - iE_2\sin\theta) & V_u - \hbar\omega \end{pmatrix} + \mu S(t)\begin{pmatrix} 0 & (E_1\cos\theta + iE_2\sin\theta)e^{-2i\omega t} \\ (E_1\cos\theta + iE_2\sin\theta)e^{+2i\omega t} & 0 \end{pmatrix}$$

Following the rotating wave approximation (RWA), after neglecting non-resonant high frequency terms, we obtain the matrix

$$V_{RWA} = \begin{pmatrix} V_g & \mu S(t)(E_1\cos\theta - iE_2\sin\theta) \\ \mu S(t)(E_1\cos\theta - iE_2\sin\theta) & V_u - \hbar\omega \end{pmatrix}$$

with eigenvalues or LIPs,

$$V_\pm = \frac{V_g + V_u - \hbar\omega}{2} \pm \frac{1}{2}\sqrt{(V_g + \hbar\omega - V_u)^2 + 4\mu^2S^2(t)|E_1\cos\theta - iE_2\sin\theta|^2} \qquad (5)$$

We can address different polarization through this last expression, such as the linearly polarized field, *e.g.* in the $z$ direction ($E_2 = 0$)

$$V_\pm^l = \frac{V_g + V_u - \hbar\omega}{2} \pm \frac{1}{2}\sqrt{(V_g + \hbar\omega - V_u)^2 + 4\mu^2S^2(t)E_1^2\cos^2\theta}$$

In this case, these dressed potentials show bond-hardening in the excited state and bond-softening in the ground state except in the surroundings of $\theta = \pm\pi/2$, where there is a LICI. The molecule dissociates through the LICI if the molecular axis rotates perpendicular to the field. The dependence of $V_\pm^l$ on $\theta$ explains that any wave packet will be subject to a torque. The direction of the torque toward the LICI or anti-alignment effect is due to the polarization in the excited state, and it was numerically predicted even when the molecule has a permanent dipole (as in $HD^+$).[6] The consequence is that any vibrational wave function created in $V_+^l$ will dissociate in the time-scale of a molecular rotation: the potential does not bare any bound state.

In similar lines, setting $E_1 = E_2$ in eqn (5), we obtain the dressed potentials for an anti-clockwise polarized field

$$V_\pm^c = \frac{V_g + V_u - \hbar\omega}{2} \pm \frac{1}{2}\sqrt{(V_g + \hbar\omega - V_u)^2 + 4\mu^2S^2(t)E_1^2} \qquad (6)$$

We obtain the same result for a clockwise circularly polarized field by choosing $E_1 = -E_2$. Note that these dressed potentials do not depend on the angle: there is no LICI that connects the excited (bond-hardened) dressed potential $V_+^c$ with the ground (bond-softened) potential $V_-^c$, so that any vibrational wave packet in $V_+^c$ remains trapped in the potential. There is also no angular dependence in this electronic state.

## 3 Numerics: quantum model of the hydrogen molecular cation under time-dependent fields

To model the dynamics of a hydrogen molecular ion under a time-dependent field, we will include electronic, vibrational and rotational degrees of freedom treated in a fully quantum way, to account for the correlation of the different degrees of freedom and the effect of decoherence that one motion can induce in the others. On the other hand, to reduce the dimensionality of the system, we study the dynamics of the molecules that lie in the plane perpendicular to the axis of propagation of the field.

Following the procedure shown in ref. 6, we solve numerically the TDSE in the position representation (discretized in a grid), given by

$$i\frac{\partial}{\partial t}\Psi(\mathbf{R},\mathbf{r}) = \left[-\frac{1}{2\mu_{ab}R}\frac{\partial}{\partial R}R\frac{\partial}{\partial R} - \frac{1}{2\mu_{ab}R^2}\frac{\partial^2}{\partial\theta^2} - \frac{1}{2}\nabla_r^2 + V(\mathbf{R},\mathbf{r}) + \mathbf{E}(t)\cdot\mathbf{r}\right]\Psi(\mathbf{R},\mathbf{r}) \qquad (7)$$

where $R$ is the internuclear distance, $\theta$ the angle between the molecular axis and the field, and $\mathbf{E}$ the field. This equation treats the electron in three degrees of freedom and includes vibration and rotation. Henceforth, it will be written as a (3 + 2)TDSE.

 

Notice also that in the dynamics we do not neglect any non-resonant (or counter-rotating) term in the field. To solve the (3 + 2) TDSE, we use the following expansion into electronic states:

$$\Psi(\mathbf{R},\mathbf{r}) = \sqrt{R}\sum_n \phi_n(R,\theta)\psi_n(\mathbf{r})$$

Considering this, eqn (7) becomes

$$i\frac{\partial}{\partial t}\varphi_n(R,\theta) = \left[-\frac{1}{2\mu_{ab}}\frac{\partial^2}{\partial R^2} - \frac{1}{8\mu_{ab}R^2} - \frac{1}{2\mu_{ab}R^2}\frac{\partial^2}{\partial\theta^2}\right]\phi_n(R,\theta) + \sum_{n'}\langle\psi_n|H_e(R,\theta,\mathbf{E}(t))|\psi_{n'}\rangle\phi_{n'}(R,\theta) \quad (8)$$

where $H_e(R, \theta, \mathbf{E}(t))$ is the electronic Hamiltonian and $\phi_n$ is the nuclear wave function in the electronic state $\psi_n$. To avoid solving for the eigenfunctions of $H_e(R, \theta, \mathbf{E}(t))$ at each grid-point, we take the eigenfunctions for $R_1 = 2a_0$,

$$H_e(R, \theta, 0)\varphi_n(R = R_0; \mathbf{r}) = H_{e,n}\varphi_n(R = R_1; \mathbf{r})$$

and then we re-scale the states in the following way:

$$\psi_n(\mathbf{r}) = \varphi_n\left(R = R_1; \mathbf{r}\frac{R}{R_1}\right)$$

In this way, we can calculate the matrix elements $\langle\psi_n|H_e(R, \theta, \mathbf{E}(t))|\psi_{n'}\rangle$ as a function of $R$, $\theta$, and $\mathbf{E}(t)$. To calculate the eigenfunctions for $R_1 = 2a_0$, we use the well-established prolate spheroidal treatment for an electron in a two-center molecule.[55–57]

Finally, we solve eqn (8) by propagating all nuclear wave functions $\phi_{n'}(R, \theta)$ over a grid of 128 points between $R = 0.1a_0$ and $R = 10a_0$, and 32 points between $\theta = -\pi$ and $\theta = \pi$, using a Strang method with a three operator-splitting scheme.[58,59]

# 4 Results

## 4.1 The ground state of circularly polarized light-induced potentials

In this section we study the nature of the light-induced potential created by a strong field of circular polarization, which we call a CLIP. We will do so by characterizing its fundamental vibro-rotational state and other states near its equilibrium geometry. First, we calculate the CLIPs. For that, we employ eqn (6). For the examples in this work, we choose $E_1 = E_2 = 0.02$ a.u. and $\omega = 0.1$ a.u. The field amplitude controls the strength of the bond hardening, and the frequency, the position of the minimum. These parameters are within the range of values where one can typically observe bond hardening in light-induced potentials, avoiding substantial ionization. To have enough intensity, in practice, most experiments are performed with 800 nm lasers and the dressing is achieved by the action of one and three photons. In this work we avoid these complications by choosing a larger frequency. The CLIPs are shown in Fig. 2, As observed, the ground CLIP $V^c_-$ exhibits bond softening, while the excited CLIP $V^c_+$ exhibits bond hardening, with a minimum at $R_0 \approx 4.1a_0$ that in principle supports several bound states. Both curves are separated by an avoided crossing near the minima with an energy gap of $\sim$0.19 a.u.

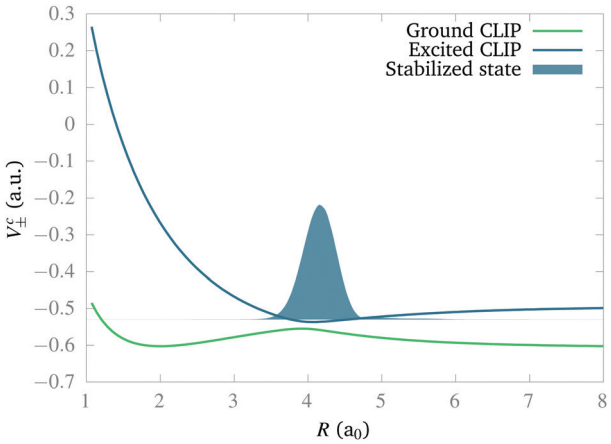


Fig. 2 Ground and excited light-induced potentials created by a strong field of circular polarization (CLIPs) with $\omega = 0.1$ a.u. and $E_1 = E_2 = 0.02$ a.u. as a function of the internuclear distance. The curves do not depend on $\theta$. Also shown is the ground vibrational wavefunction in the excited CLIP. Note that the CLIPs exhibit bond hardening, bond softening and an avoided crossing for all values of the angle.

Then, we need to isolate the ground vibrational state of the excited CLIP. To do so, we will use a dynamic approach, by propagating an initial Gaussian wave packet in a linear combination of the ground and excited electronic states centered at $R_0$, under a circularly polarized field, adding an artificial imaginary potential at small and large internuclear distances, namely,

$$V_{\mathrm{im}}(R) = \begin{cases} -i/10(R - R_{\mathrm{min}})^2 & \text{if } R < R_{\mathrm{min}} = 2a_0 \\ -i/10(R - R_{\mathrm{max}})^2 & \text{if } R < R_{\mathrm{max}} = 7a_0 \\ 0 & \text{elsewhere} \end{cases} \quad (9)$$

Because we expect no angular dependence in the CLIP (see Section 2), we can set the initial wave packet with an arbitrary angular distribution. While running the dynamics, we observe that some of the population dissociates or transits to lower internuclear distances, and in both cases, vanishes due to the imaginary potential. As long as the imaginary potential filters contributions from dissociative states (for large $R$) and the ground state (for small $R$), the particular parameters of the imaginary potential do not affect the asymptotic state wave function that is finally obtained, but the time needed to reach it. For our chosen parameters (see eqn (9)), what is left after 100 fs is approximately the ground vibrational state of $V^c_+$. In Fig. 2, we show such wave packet at the end of the dynamics along with the ground and excited CLIPs (see eqn (6)), and we can observe that the outcome matches approximately the minimum of the excited CLIP. We achieve the same results for different starting angular distributions. In particular, in the plot a uniform distribution was used, but the final radial wave function did not depend on the angle.

Naturally, the question is why the dynamics works to find the ground vibrational state of the excited CLIP. The answer is that our simulations show that this state is not stable (as expected

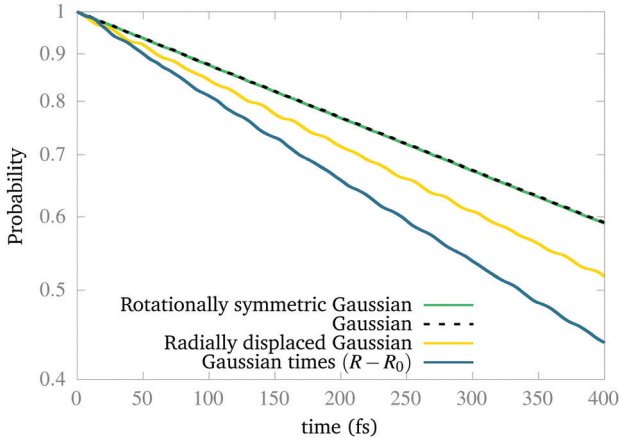


Fig. 3 Population decay in the presence of a circularly polarized field for a set of different initial wave packets initially created in $V_+^c$, measured as the norm of the wave function in the grid.

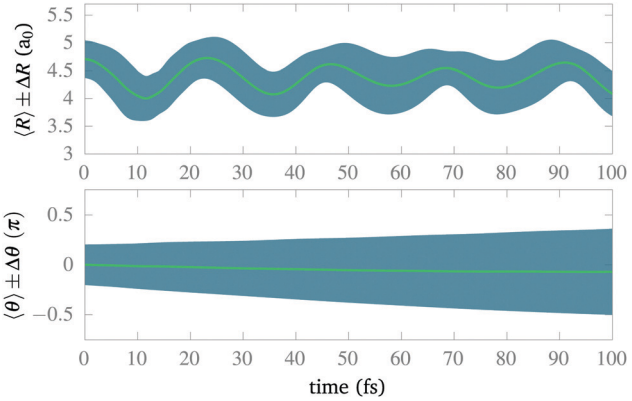


Fig. 4 Time evolution of the expected bond length $R(t)$, the expected angle between the field $\mathbf{E}_1$ and the molecular axis $\theta(t)$, and their corresponding standard deviations, in the presence of a circularly polarized field with $\omega$ = 0.1 a.u. and $E_1 = E_2$ = 0.02 a.u. The initial wave function corresponds to a Gaussian in $R$ displaced $0.5a_0$ from $R_0$, times a Gaussian in $\theta$ with $\sigma_\theta = 0.2\pi$.

from the model in Section 2) but metastable. Indeed, a wave packet can remain in the excited CLIP for an appreciable time (*e.g.* during several vibrational periods) while dissociating slowly. But as the wave packet sits or moves around the avoided crossing, there is a non-negligible probability of crossing to the lowest CLIP by non-adiabatic coupling, induced by the kinetic term, which we did not include in the model. Henceforth, the ground vibrational state is the one that remains after a relatively long dynamics. To test this, in Fig. 3, we create the system in different initial states and calculate the remaining population as a function of time. As we can observe, the population in all cases of study decays exponentially, as one can expect from a metastable state. In particular, the wave packets that are initially Gaussian in the radial coordinate, resembling the expected vibrational ground state, are the most slowly decaying, independent of the angular distribution. In contrast, a Gaussian displaced to larger bond distances or a function created as a Gaussian times a linear-term, resembling the first excited vibrational state, decays faster. Finally, we must remark that the initial state, created as a superposition of the ground and excited electronic states by hand, initially decays faster due to transient effects (the electronic components of the wave function are not similar to those of the true electronic eigenfunction of the dressed Hamiltonian) that are filtered during the first stage of the dynamics, before reaching the slow exponential-decay regime. Only after reaching this steady regime we consider that the wave functions obtained are the vibrational and electronic eigenstates (or electronic eigenstates times a nuclear wave packet) that we show in the paper.

### 4.2 Dynamics and metastability

After isolating the vibrational ground state, we now proceed to study its stability and the stability of the CLIP in the proximity of the equilibrium geometry. From now on, we remove the imaginary potential for low internuclear distances, allowing the system to be in the ground electronic state. In Fig. 4, we show the average and standard deviation in $R$ and $\theta$ under a circularly polarized field for a nuclear wave packet that is the ground state displaced by $0.5a_0$ ($\sim 1.5\sigma_R$, where $\sigma_R$ is the standard deviation of the initial state in the radial direction). Likewise, we choose a Gaussian wave packet in the angle, centered at $\theta = 0$ with width $\sigma_\theta = 0.2\pi$. As expected, we observe vibrations in the LIP with a 23 fs period during the 100 fs of simulation with a fairly constant standard deviation (although slightly increasing because of dephasing and dissociating fragments), indicating a high degree of stability. In the angle, the average remains the same as there is no torque, but the packet naturally spreads as the potential is flat on $\theta$ (it does not depend on the angle). The spreading in the angle is slower than in $R$ as the rotational quantum is smaller than the vibrational one.

In Fig. 5, we present some snapshots from the first period of oscillation of the wave packet dynamics considered in Fig. 4. The dynamics shows the typical vibration of the packet, where it spreads mostly at the classical turning points, and squeezes in the initial position, characteristic of harmonic motion. However, we also observe the gradual emergence of a second maximum due to the anharmonic nature of the CLIP. At certain times, the spreading enlarges due to the dissociation of small components of the packet (for instance, at $t$ = 11.25 fs, around $\theta = 0$, $R = 6a_0$). The slow decay of population to $V_-^c$ leads to photodissociation in the excited electronic state, $V_2$, as both curves correlate at large $R$ (see Fig. 2). The electronic population dynamics is subtle. The CLIP is created by the periodic electron dynamics induced by the circularly polarized field, but the dynamics is no longer periodic when the nuclei move. Consequently, the electron loses its synchronization with the field and the wave function is no longer in the exact mix of the ground and first excited electronic states that creates the CLIP. Indeed, the circularly polarized field period is of the order of 1 fs, which is not that far from the timescale of the nuclear dynamics, so the electron cannot instantly adapt to the movement.

### 4.3 Analysis of photofragments

So far, we have explored the nature of the CLIPs and concluded that they sustain a metastable state that slowly dissociates. One question that remains is what happens with the

 

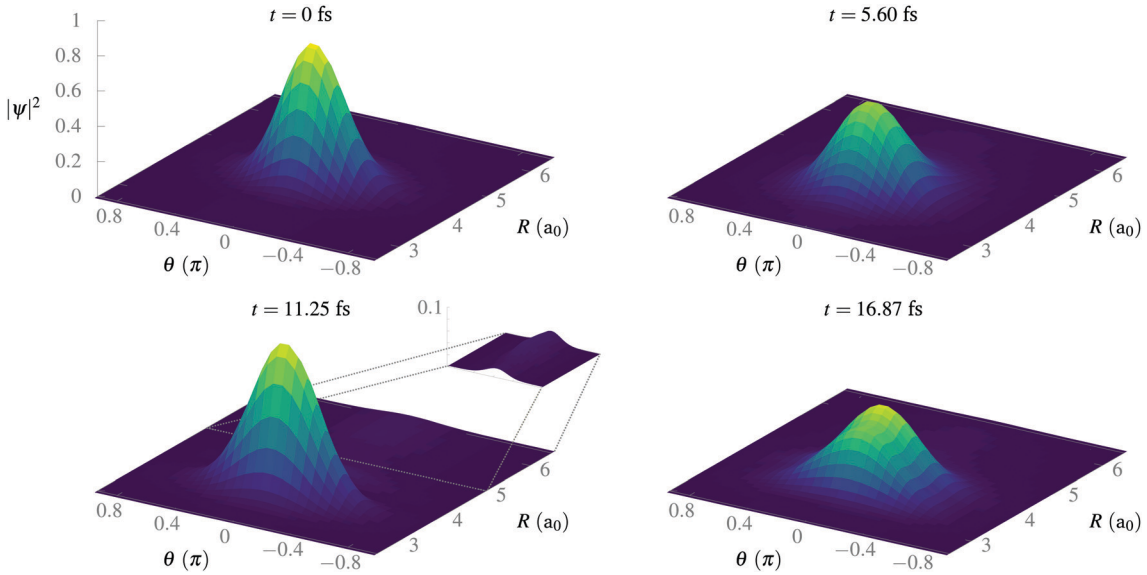


Fig. 5 Snapshots of the time evolution of a Gaussian wave packet initially displaced $0.5a_0$ from $R_0$, with $\sigma_R = 0.34a_0$ and $\sigma_\theta = 0.2\pi$ in the presence of a circularly polarized field.

dissociating fragments of the wave packet. Can the amplitudes of the linearly polarized fields that create the circular polarization be modified to observe the fingerprints of other effects, such as the anti-alignment with the field in the excited electronic state? To explore this, we created a wave packet with a Gaussian distribution in $R$ and $\theta$, centered approximately at $R_0$ and $\theta = 0$. Then, we solved the TDSE with circularly, elliptically, and linearly polarized fields. Finally, we compared the final angular distribution of the dissociating fragments. We calculate the photo-angular distribution (PAD) in the following way:

$$\Gamma = \int_0^t \mathrm{d}t \int_0^\infty \mathrm{d}\mathbf{r} \int_{R_1}^{R_2} \mathrm{d}R |\Psi(\mathbf{R}, \mathbf{r}, \mathbf{t})|^2$$

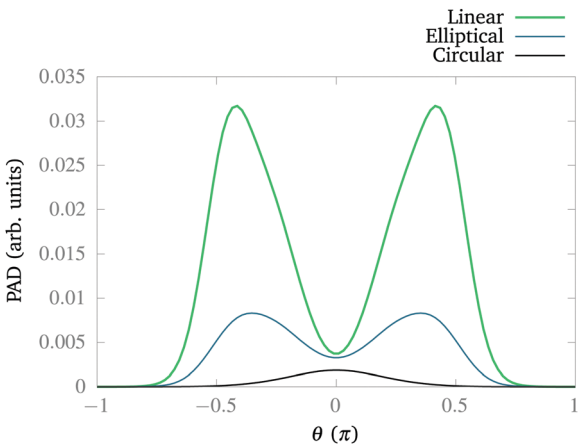


Fig. 6 Angular distribution of the dissociating fragments for linear, elliptical, and circular polarization after 10 fs of simulation. The integral is taken from $R_1 = 6a_0$ to $R_2 = 10a_0$. We use $E_1 = 0.02$ a.u. and $E_2 = 0.01$ a.u. for the elliptically polarized case, $E_1 = 0.04$ and $E_2 = 0$ for the linearly polarized case, and $E_1 = E_2 = 0.02$ a.u. for the circularly polarized case. In all these cases, we set $\omega = 0.1$ a.u.

where $R_1$ is set to $6a_0$ in order to ignore the stabilized part of the wavepacket and $R_2$ is set to $10a_0$, the boundary of the simulation. In practice, we observed that the shape of the PADs does not strongly depend on time after the first $\sim$10 fs so that there is no need to integrate over time except to obtain the exact yields, which can be easily inferred from the norm of the wave function.

In Fig. 6, we present the distribution for the three cases. First, we can observe that the linear polarization dissociates more strongly than the other two cases, followed by the elliptical case. Second, the elliptical and linear cases show maxima around $\theta \pm \pi/2$ indicating anti-alignment, as we expected from the corresponding CLIPs. Note that the maxima are displaced because a fragment has to travel from $\theta = 0$, the position of the wave packet. Finally, for the circular polarization, the fragments just travel radially, as observed in Fig. 5. Typically, the anti-alignment and subsequent photodissociation with linearly or elliptically polarized fields is faster than the dissociation through non-adiabatic couplings that induce the metastability of the wave packets in the CLIP.

## 5 Conclusions

Excited states of single-electron molecules are unstable under strong linearly polarized laser pulses. In spite of bond-hardening, due to the polarizability of the molecule (the effect of a charge transfer that creates a transient dipole that increases linearly with the internuclear distance), the same polarizability is responsible for anti-alignment, leading to fragmentation at perpendicular orientations of the polarization vector in the excited state.

Under the effect of circularly polarized fields, we have shown that the light-induced potential does not show any light-induced conical intersection. Bond hardening allows the wave packet to sustain vibrational motion in the LIP. The LIP is

independent of the angle, so an initial rotational wave packet slowly disperses in the flat potential at a rate inversely proportional to the moment of inertia. Due to non-adiabatic couplings, the vibrational motion leads to a slow decay in the continuum, so that all eigenstates of the CLIP are meta-stable. However, the states survive for a few hundreds of femtoseconds, enough to allow for many different quantum control actions.

In this work we have shown the results for constant one-color fields, but the emerging picture clearly indicates what will be the main results when using ultrashort femtosecond pulses. Initially, we expect some steeper decay in the population as the pulse amplitude increases and before the electronic populations adjust to the LIP. If the pulse is slow, then the wave packet will adiabatically change adapting to the LIP. Then, depending on the polarizability of the field, either the molecule will anti-align and dissociate or the molecular axis will remain at its initial state, where the molecule slowly dissociates. We have identified the simplest experimental observable to distinguish both situations, namely the photofragment angular distributions. We believe that previous experiments may show indications of anti-alignment.[60] A more thorough study of these dynamical effects will be explored in future studies and we hope to motivate further experiments using both linearly and circularly polarized pulses to control the photodissociation of simple molecules.

## Conflicts of interest

There are no conflicts to declare.

## Acknowledgements

This work was supported by the Army Research Laboratory under Cooperative Agreement Numbers W911NF-21-2-0037 (S. C.), National Agency for Research and Development (ANID) under Fondecyt Award No. 1190703 (J. A. V.), Fondecyt Award No. 1190662 (J. R.), and CEDENNA through ''Financiamiento Basal para Centros Científicos y Tecnológicos de Excelencia'' under Award No. AFB180001 (J. R. and J. A. V.), the Quantum Computing Technology Development Program (NRF-2020M3E4A1079793) (B. Y. C.) and MINECO CTQ2015-65033-P (I. R. S.).

## Notes and references

1 S. A. Rice and M. Zhao, *Optical Control of Molecular Dynamics*, Wiley, 2000.
2 M. Shapiro and P. Brumer, *Principles of the Quantum Control of Molecular Processes*, Wiley & Sons, Hoboken, 2003.
3 C. Brif, R. Chakrabarti and H. Rabitz, in *Control of quantum phenomena*, ed. S. A. Rice and A. R. Dinner, Wiley-Blackwell, 2012, vol. 148, pp. 1–76.
4 G. A. Worth and G. W. Richings, *Annu. Rep. Prog. Chem., Sect. C: Phys. Chem.*, 2013, **109**, 113–139.
5 I. R. Sola, B. Y. Chang, S. A. Malinovskaya and V. S. Malinovsky, in *Chapter Three - Quantum Control in Multilevel Systems*, ed. E. Arimondo, L. F. DiMauro and S. F. Yelin, Academic Press, 2018, vol. 67 of Advances In Atomic, Molecular, and Optical Physics, pp. 151–256.
6 S. Carrasco, J. Rogan, J. A. Valdivia and I. R. Sola, *Phys. Chem. Chem. Phys.*, 2021, **23**, 1936–1942.
7 P. H. Bucksbaum, A. Zavriyev, H. G. Muller and D. W. Schumacher, *Phys. Rev. Lett.*, 1990, **64**, 1883–1886.
8 A. Zavriyev, P. H. Bucksbaum, H. G. Muller and D. W. Schumacher, *Phys. Rev. A: At., Mol., Opt. Phys.*, 1990, **42**, 5500–5513.
9 B. Yang, M. Saeed, L. F. DiMauro, A. Zavriyev and P. H. Bucksbaum, *Phys. Rev. A: At., Mol., Opt. Phys.*, 1991, **44**, R1458–R1461.
10 S. W. Allendorf and A. Szöke, *Phys. Rev. A: At., Mol., Opt. Phys.*, 1991, **44**, 518–534.
11 A. Giusti-Suzor and F. H. Mies, *Phys. Rev. Lett.*, 1992, **68**, 3869–3872.
12 G. Yao and S.-I. Chu, *Chem. Phys. Lett.*, 1992, **197**, 413–418.
13 A. Zavriyev, P. H. Bucksbaum, J. Squier and F. Saline, *Phys. Rev. Lett.*, 1993, **70**, 1077–1080.
14 E. E. Aubanel, J.-M. Gauthier and A. D. Bandrauk, *Phys. Rev. A: At., Mol., Opt. Phys.*, 1993, **48**, 2145–2152.
15 B. Y. Chang, H. Rabitz and I. R. Sola, *Phys. Rev. A: At., Mol., Opt. Phys.*, 2003, **68**, 031402.
16 B. Y. Chang, S. Lee and I. R. Sola, *J. Chem. Phys.*, 2004, **121**, 11118–11128.
17 I. R. Sola, *Phys. Rev. A: At., Mol., Opt. Phys.*, 2004, **69**, 033401.
18 B. Y. Chang, S. Shin and I. R. Sola, *Phys. Rev. A: At., Mol., Opt. Phys.*, 2010, **82**, 063414.
19 B. Y. Chang, S. Shin, A. Palacios, F. Martn and I. R. Sola, *ChemPhysChem*, 2013, **14**, 1405–1412.
20 G. G. Balint-Kurti, S. Zou and A. Brown, in *Optimal Control Theory for Manipulating Molecular Processes*, ed. S. A. Rice and A. R. Dinner, John Wiley & Sons, Inc., 2008, vol. 138, pp. 43–94.
21 B. Y. Chang, S. Shin, A. Palacios, F. Martn and I. R. Sola, *J. Chem. Phys.*, 2013, **139**, 084306.
22 B. Y. Chang, S. Shin, A. Palacios, F. Martn and I. R. Sola, *J. Phys. B: At., Mol. Opt. Phys.*, 2015, **48**, 043001.
23 B. Y. Chang, S. Shin, J. Santamaria and I. R. Sola, *J. Chem. Phys.*, 2009, **130**, 124320.
24 B. Y. Chang, S. Shin and I. R. Sola, *J. Chem. Phys.*, 2009, **131**, 204314.
25 M. E. Corrales, J. Gonzalez-Vazquez, G. Balerdi, I. R. Sola, R. de Nalda and L. Bañares, *Nat. Chem.*, 2014, **6**, 785.
26 M. E. Corrales, R. de Nalda and L. Bañares, *Nat. Commun.*, 2017, **8**, 1345.
27 H. Stapelfeldt and T. Seideman, *Rev. Mod. Phys.*, 2003, **75**, 543–557.
28 T. Seideman and E. Hamilton, *Adv. At., Mol., Opt. Phys.*, 2005, **52**, 289–329.
29 B. Y. Chang, S. Shin, J. González-Vázquez, F. Martn, V. S. Malinovsky and I. R. Sola, *Phys. Chem. Chem. Phys.*, 2019, **21**, 23620–23625.
30 J. Yuan and T. F. George, *J. Chem. Phys.*, 1978, **68**, 3040–3052.
31 A. D. Bandrauk and M. L. Sink, *J. Chem. Phys.*, 1981, **74**, 1110–1117.

 

32 B. M. Garraway and K. A. Suominen, *Phys. Rev. Lett.*, 1998, **80**, 932–935.
33 I. R. Sola, B. Y. Chang, J. Santamaria, V. S. Malinovsky and J. L. Krause, *Phys. Rev. Lett.*, 2000, **85**, 4241–4244.
34 P. Emil, B. Joachim and G. Stefanie, *New J. Phys.*, 2009, **11**, 105035.
35 B. Y. Chang, I. R. Sola and S. Shin, *Int. J. Quantum Chem.*, 2016, **116**, 608–621.
36 N. Moiseyev, M. Šindelka and L. S. Cederbaum, *J. Phys. B: At., Mol. Opt. Phys.*, 2008, **41**, 221001.
37 G. J. Halász, M. Šindelka, N. Moiseyev, L. S. Cederbaum and Á. Vibók, *J. Phys. Chem. A*, 2012, **116**, 2636–2643.
38 P. V. Demekhin and L. S. Cederbaum, *J. Chem. Phys.*, 2013, **139**, 154314.
39 G. J. Halász, Á. Vibók and L. S. Cederbaum, *J. Phys. Chem. Lett.*, 2015, **6**, 348–354.
40 A. Csehi, G. J. Halász, L. S. Cederbaum and A. Vibók, *J. Phys. Chem. Lett.*, 2017, **8**, 1624–1630.
41 C. Fábri, B. Lasorne, G. J. Halász, L. S. Cederbaum and Á. Vibók, *J. Phys. Chem. Lett.*, 2020, **11**, 5324–5329.
42 M. Auzinsh, D. Budker and S. Rochester, *Optically polarized atoms: understanding light-atom interactions*, Oxford University Press, 2010.
43 Z. B. Rudzikas, A. A. Hikitin and A. F. Kholtygin, *Leningrad Izdatel Leningradskogo Universiteta*, 1990.
44 M. Ivanov, P. Corkum, T. Zuo and A. Bandrauk, *Phys. Rev. Lett.*, 1995, **74**, 2933.
45 N. Böwering, T. Lischke, B. Schmidtke, N. Müller, T. Khalil and U. Heinzmann, *Phys. Rev. Lett.*, 2001, **86**, 1187.
46 C. Lux, M. Wollenhaupt, T. Bolze, Q. Liang, J. Köhler, C. Sarpe and T. Baumert, *Angew. Chem., Int. Ed.*, 2012, **51**, 5001–5005.
47 P. V. Demekhin, A. N. Artemyev, A. Kastner and T. Baumert, *Phys. Rev. Lett.*, 2018, **121**, 253201.
48 R. E. Goetz, C. P. Koch and L. Greenman, *Phys. Rev. Lett.*, 2019, **122**, 013204.
49 Y. Fujimura, L. González, K. Hoki, J. Manz and Y. Ohtsuki, *Chem. Phys. Lett.*, 1999, **306**, 1–8.
50 M. Shapiro, E. Frishman and P. Brumer, *Phys. Rev. Lett.*, 2000, **84**, 1669.
51 D. V. Zhdanov and V. N. Zadkov, *Phys. Rev. A: At., Mol., Opt. Phys.*, 2008, **77**, 011401.
52 C. Chen, J. Wu and H. Zeng, *Phys. Rev. A: At., Mol., Opt. Phys.*, 2010, **82**, 033409.
53 T. Brixner, G. Krampert, T. Pfeifer, R. Selle, G. Gerber, M. Wollenhaupt, O. Graefe, C. Horn, D. Liese and T. Baumert, *Phys. Rev. Lett.*, 2004, **92**, 208301.
54 D. Ayuso, O. Neufeld, A. F. Ordonez, P. Decleva, G. Lerner, O. Cohen, M. Ivanov and O. Smirnova, *Nat. Photonics*, 2019, **13**, 866–871.
55 M.-G. Baik, M. Pont and R. Shakeshaft, *Phys. Rev. A: At., Mol., Opt. Phys.*, 1996, **54**, 1570.
56 G. L. Kamta and A. Bandrauk, *Phys. Rev. A: At., Mol., Opt. Phys.*, 2004, **70**, 011404.
57 G. L. Kamta and A. D. Bandrauk, *Phys. Rev. A: At., Mol., Opt. Phys.*, 2005, **71**, 053407.
58 T. Sørevik, T. Birkeland and G. Okša, *J. Comput. Appl. Math.*, 2009, **225**, 56–67.
59 R. I. McLachlan and G. R. W. Quispel, *J. Phys. A: Math. Gen.*, 2006, **39**, 5251.
60 M. Kübel, M. Spanner, Z. Dube, A. Y. Naumov, S. Chelkowski, A. D. Bandrauk, M. J. Vrakking, P. B. Corkum, D. Villeneuve and A. Staudte, *Nat. Commun.*, 2020, **11**, 1–8.